PETRA III Extension Project

Beamline P24 — Chemical Crystallography

Technical Design Report

June 26, 2014

Contributors

DESY Photon Science, FS-PEX

Martin Tolkiehn	Workpackage Leader
Heiko Schulz-Ritter	Beamline Engineer
Wolfgang Drube	PETRA III Extension Project Leader

University Hamburg, Mineralogy Department

Carsten Paulmann	Beamline Scientist
Andreas Berghäuser	Engineer
Dennis Ropers	Engineer

Chapter 1

Introduction and overview

1.1 PETRA III extension project

DESY is one of the world's leading accelerator centers and a member of the Helmholtz Association, Germany's largest scientific research organization comprising 18 scientific- technical and biological-medical research centers. It develops, builds and operates large particle accelerators used to investigate the structure of matter. Photon science is a major branch of its research activities and DESY has a long standing tradition in the use of synchrotron radiation. For almost 38 years, the 2^{nd} generation facility DORIS served as a very productive high-flux source for synchrotron radiation based research until it was finally shut down in October 2012. Currently, the main photon sources at DESY are the storage ring PETRA III and the Free-Electron-Laser FLASH, offering unique research possibilities for an international scientific community.

PETRA III is a low-emittance (1 nmrad) 6 GeV storage ring having evolved from the conversion of the large PETRA accelerator into a 3^{rd} generation light source. Construction started in 2007 and first beamlines became operational in 2009. Today, a total of 14 undulator beamlines are in user operation in the "Max-von-Laue" experimental hall covering 1/8 of the storage ring.

The focus of the facility is on applications making optimum use of the high beam brilliance especially at hard x-ray energies, i.e. experiments aiming at nano focusing, ultra-high resolution studies and coherence applications. Because a number of very productive techniques formerly available at DORIS III are not currently implemented at PETRA III and the user demand for access to the new beamlines was anticipated to be very high, it was decided to extend the experimental facilities at the new source and to provide additional beamlines. This PETRA III extension project adds two new experimental halls on either side (North and East) of the current "Max-von-Laue Hall" making use of the long straight sections

and part of the adjacent arcs (see Fig. 1.1)

The northern straight section accommodates one of two 40 m long damping wiggler arrays producing an extremely hard and powerful x-ray beam which will also be utilized for materials science experiments. The long straight section in the east is available for additional insertion devices.

In order to accommodate insertion device sources in the arc sections, which are filled with long dipole magnets yielding a rather soft X-ray spectrum, the machine lattice will be modified. The new lattice adds double bent achromat (DBA) cells in the arcs, each allowing for a 5 m long straight section. Similar to the present PETRA III beamlines, these straights will serve two beamlines independently by use of canting dipoles resulting in two separate 2 m long straights. Different from the present 5 mrad canting scheme, a canting angle of 20 mrad was chosen at the extension beamlines to provide more spatial flexibility for the experiments further downstream. In total, the new lattice provides eight short straight sections in the two arcs with source properties corresponding to a high-beta section at PETRA III making them very suitable for the use of undulators.

Some of the new beamlines will be designed as ”short undulator” beamlines continuing most of the productive techniques formerly provided at DORIS III bending magnet beamlines. These sources will not only be very well suited for the spectrum of applications to be relocated from DORIS III but also provide a

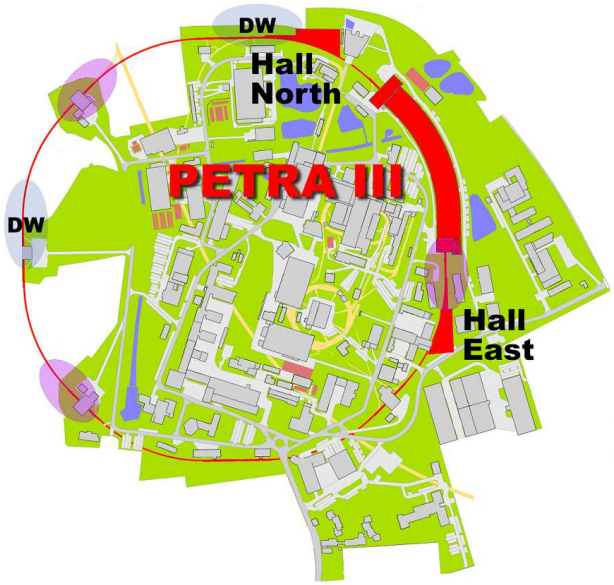

Figure 1.1: View of the PETRA III storage ring (red line). The present experimental hall is shown together with the additional experimental halls in the North and East which are currently under construction.

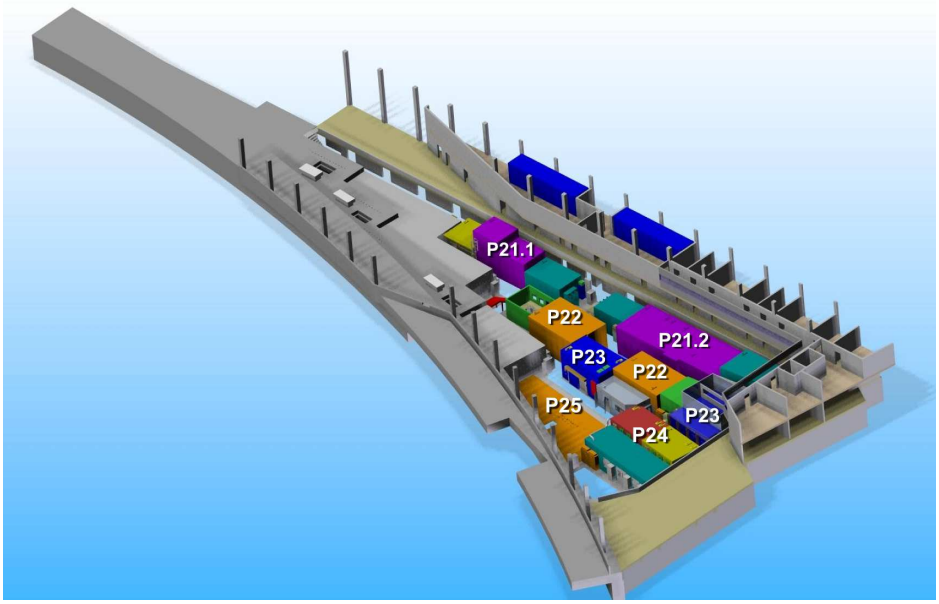

Figure 1.2: Beamlines in PETRA III hall East.

considerably brighter beam. In addition, high-brilliance long undulator beamlines will be built, three in collaboration with international partners, Sweden, India and Russia which will all be located in PETRA III hall East.

Since 2009, the science case as well as specifications of the techniques to be implemented are being discussed with the user community, scientific advisory bodies and international partners. A number of specific user workshops have been held. A critical issue is the timing of the construction of the extension project because its realization requires a complete shutdown of the current PETRA III user facility for an extended period of time. Also, a prioritization scheme has been defined for a successive implementation of the new beamlines in three phases (see Table 1.1). Phase 1 beamlines P64/65 (X-ray absorption spectroscopy) are planned to become operational in Fall 2015.

The civil construction of the PETRA III extension started in February, 2014. During the machine modifications and the initial construction phase of the experi-

Phase 1	Beamlines P64, P65
Phase 2	Beamlines P21, P22, P23, P24
Phase 3	Beamlines P61, P66
Not yet funded	Beamlines P25, P62, P63

Table 1.1: Development phases of the PETRA III extension project.

mental halls, the storage ring cannot be operated and the user operation at PETRA III will pause. Every effort is therefore being made to minimize this interruption. The completion of the new facilities PETRA III North and East will continue in parallel to the user operation at the present beamlines which is planned to resume in March 2015.

1.2 Scientific case

The final shutdown of DORIS III discontinued some successful experimental stations (D3, F1, B2) which served as 'workhorse' beamlines for crystallographic applications coming from different scientific fields like physics, chemistry as well as material and earth sciences and biology. Typical applications covered classical crystal structure studies, diffuse scattering studies, charge density analysis, phase transitions, disordered and modulated structures all at ambient and non-ambient conditions. The purpose of the planned beamline P24 is the continuation of these applications and to provide a powerful instrument for new applications, which will make use of the superior properties of PETRA III. As these techniques have different and partly conflicting demands, their realization requires two experimental hutches with different diffractometers. One of these hutches will be build in cooperation with University Hamburg and the BMBF (Federal Ministry of Education and Research) joint research project 'Chemical Crystallography'. The other hutch will be the new home of the Huber four circle diffractometer with Eulerian cradle, that was used at the DORIS III beamline D3.

1.2.1 The BMBF joint research project 'Chemical Crystallography'

As a result of the Petra III Extension Workshop in November 2009, a collaboration of different university groups formed to expedite funding and instrumentation of an experimental station dedicated to crystallographic research fields which require photon flux but not ultimate brilliance like the current PETRA III beamlines. An increasing number of novel compounds form extremely small crystals unsuitable even for the most intense X-ray generators equipped with focussing optics. In addition, compounds containing heavier elements require synchrotron radiation energies beyond common available laboratory X-ray radiation sources. The joint research funding for engineering personnel, diffractometer and further instrumentation was granted in June 2010 to the Universities Hamburg, Mnchen and Freiberg with associated members from MPI Mlheim, MPI Gttingen and University Bayreuth. The science case along with suitable design parameters were

discussed with the user community during a project member meeting in September 2011 (Salzburg) and two project-organised workshops (Hamburg) with 30–45 participants and 10–12 talks each. As a common agreement, the beamline should serve applications like:

- General diffraction experiments
- Dynamics, time-resolved crystallography
- Disordered structures
- Charge-density studies
- Phase transitions & External fields
- Photo-crystallography
- Solid-state chemistry & crystallisation

The applications demand for sufficient space for a large variety of sample environments, e.g.:

- Low/High Temperature (20 K - 1700 K)
- High pressure (DAC devices)
- Laser/Chopper system
- Digital polarising microscope
- Reaction chambers
- External fields (Stress/strain, electrical/magnetical)

along with the availability of a close-distance chemical preparation lab with integrated fume-hood including Nitrogen, Helium and Argon supply. It was decided that a diffractometer with Kappa geometry is best suited to accommodate all these sample environments.

The basic beam parameters were proposed with an energy-range $8keV$–$44keV$ with emphasis on energies above $17keV$. A standard beamsize of ca. $1.0 \cdot 1.0mm^2$ (FWHM) should provide a homogenous beamsize of at least $0.3 \cdot 0.3mm^2$ for standard applications and an option for focusing towards the micrometer range for position-resolved diffraction studies.

1.3 User workshop

The design parameters of the beamline were discussed with the potential user community including users of the DORIS III beamlines D3 and F1 and finalized in a workshop, which took place in March 2014. Table 1.2 gives an overview of the demands of the users. The most important parameters discussed at this workshop are energy range, photon flux and beamsize. For the unfocussed mode, a uniform region of $0.3mm$ diameter is required.

Besides these optical parameters also requirements for experimental infrastructure were discussed. Many users demand a sample preparation lab located very close to the instruments at the beamline. This lab should be equipped with a fume hood, so that toxic solvents can be handled. For air or moisture sensitive samples a long transport through the experimental hall must be avoided and thus the central chemical lab in the building cannot be used.

For precise temperature dependent studies at low temperatures a closed cycle cryostat is required. Such a device cannot be mounted on the Kappa diffractometer, which has been acquired by the University Hamburg. However the cryostat can easily be used with the second diffractometer, which is planned for the second experimental hutch. It is desirable that access to the second hutch is possible while an experiment in the first hutch is ongoing, so that experiments, which require complex preparatory work, can be prepared in the second hutch.

In the following chapter a design for the P24 beamline, which fulfills all these requirements, will be presented.

Beamline parameter	**User demand**
Energy range	8keV (fixed) and 15keV – 44keV (tunable)
Photon flux density	$> 10^{12} s^{-1} mm^{-2}$
Beamsize	unfocussed $\approx 1mm$ intermediate $\approx 100\mu m$ micro $< 20\mu m$
Diffractometers	• Kappa diffractometer • Four circle diffractometer with Eulerian cradle
Experimental hutches	• Two separate hutches • Sample preparation lab (with fume hood) should be located nearby • Enough space for complex sample environments (e.g. in-situ equipment) • Infrastructure for Helium and Nitrogen gas jet cryostats • Infrastructure for use of gases and other media like pressurised air and cooling water

Table 1.2: Key parameter of beamline P24

Chapter 2

Beamline Layout

Beamline P24 is located in sector 3 of hall East (see Fig. 2.1) sharing the optics hutch with beamline P25 which is not yet funded and will be built at a later stage.

The design of P24 is determined by several boundary conditions. First and most important, the demands of the user community as summarized in the previous chapter. Second, due to budgetary constraints the re-use of some instrumentation from previous DORIS III bending magnet beamlines is required, such as the double-crystal monochromator and a 4-circle diffractometer. The third boundary condition are the storage ring properties, namely the small emittance at high electron energy and the large radius, which results in large distances between the

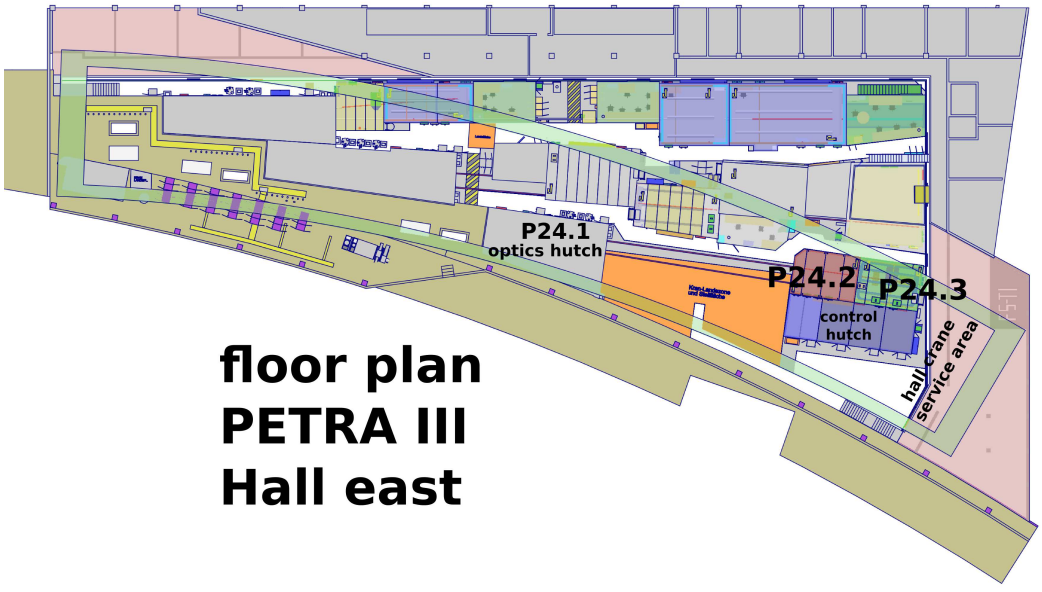

Figure 2.1: Beamlime P24 floorplan

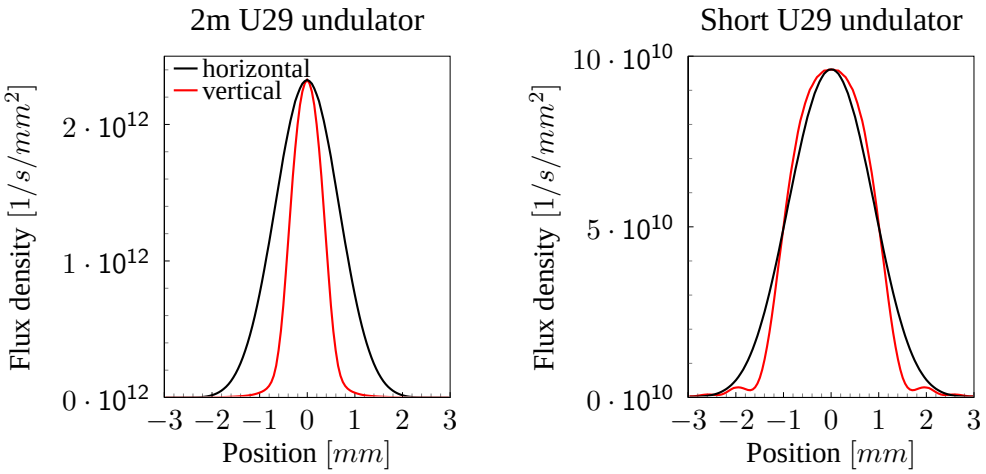

Figure 2.2: Comparison of beam profile in first experimental hutch ($80m$ away from source, $17.7keV$), assuming a Si(311) monochromator. The undulator parameters can be found in Table 2.1

source and the first optical elements. The proposed design considers all these boundary conditions.

2.1 Source

For the choice of the radiation source for P24 the most important parameter is the maximum power density allowed for the water-cooled "C-type" double-crystal monochromator, which is about $2W/mm^2$ (see section 2.2.2 for more details). The obvious solution, which fulfills this condition, is a short undulator in conjunction with two plane mirrors to cut off the higher harmonics radiation. A sim-

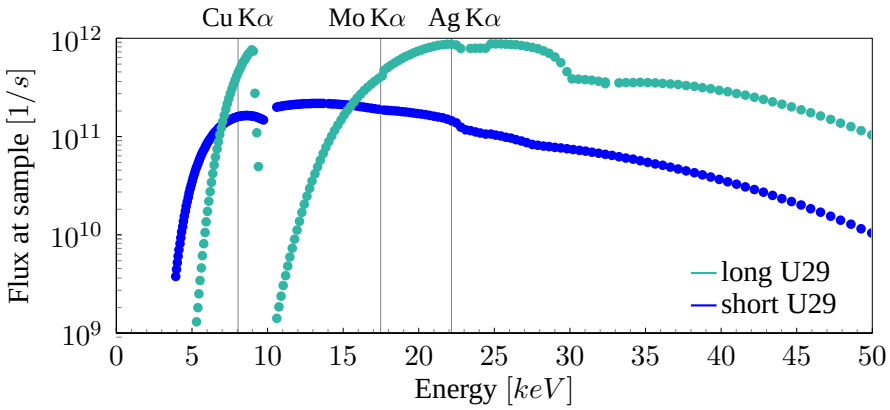

Figure 2.3: Comparison of the tuning curves of a short (11 period) and a long (2m) U29 undulator taking into account Cu attenuators, higher harmonic rejection mirrors and a Si(311) monochromator. Below $24keV$ a factor of four can be gained by switching to the Si(111) crystal pair.

ilar design was chosen by other PETRA III Extension beamlines including e.g. EXAFS beamline P65. However the demands of the potential user community of P24 and the EXAFS community are quite different: While EXAFS needs energy tunability, crystallography experiments are performed at some fixed energies. In most cases this energy is chosen well above $15keV$ and only few users, who are using a Cu source at their home institute, would like to use $8.048keV$ for their experiments. This allows the use of Cu attenuators in the beamline front end (see Fig. 2.4) to absorb the first harmonic of the undulator and thereby reduce the heat load. This way it is possible to use a standard PETRA III $2m$ long undulator. Such a design has several advantages over a short undulator: First, the radiation from a long undulator is less divergent and thus the size of the unfocussed beam will be smaller. A comparison of the horizontal and vertical beam profile for a long and a short undulator is shown in Fig. 2.2. The vertical beam size is about three times smaller for the long undulator. The second advantage of the long undulator is the higher photon flux and more importantly the higher flux density, which is more than an order of magnitude higher at $17keV$. However at energies below $\approx 15keV$ the absorption of the Cu attenuator becomes larger than the gain from the longer undulator. This can be seen from the comparison of the tuning curves shown in Fig. 2.3. For both curves the bandwith of a Si(311) monochromator and the reflectivity of the higher harmonic rejection mirrors was taken into account. For the long undulator the absorption of the Cu attenuators, that are necessary to keep the heat load below the $2W/mm^2$ limit, was also taken into account. Since at least one $50\mu m$ thick Cu absorber is always in the beam, there is a gap between $9keV$ and $15keV$ where the flux is low. This energy range, however, is not important

	Standard	**Short**
Minimum magnetic gap	$9.5mm$	
Period length λ_U	$29mm$	
Length L	$2m$	$0.32m$
Peak field B_0	$0.81T$	
Deflection parameter K_{max}	2.2	
First harmonic E_1	$3.54keV$	
Total power P_{tot}	$3.1kW$	$0.49kW$
Power in $1 \cdot 1mm^2$ at $55m$	$26W$	$4.1W$
Source size $\sigma_{Tx} \cdot \sigma_{Ty}$ ($17.7keV$)	$130 \cdot 6.5\mu m^2$	$130 \cdot 6.3\mu m^2$
Source divergence $\sigma_{Tx'} \cdot \sigma_{Ty'}$ ($17.7keV$)	$8.6 \cdot 4.6\mu$rad^2	$13 \cdot 11\mu$rad^2

Table 2.1: Parameters of the PETRA III standard X-ray undulator U29 calculated for $6.08GeV$ positron energy and $99mA$ beam current.

for most potential users and the gap can be tolerated. Finally, the long undulator design allows an easy upgrade path to a cryogenically cooled monochromator at a later time, as no changes have to be made to the beamline front end except for the removal of the Cu attenuators.

As energy scanning is not required for crystallography, no overlap of the undulator harmonics in the tuning curve is required. Therefore a standard U29 undulator (see Table 2.1) can be used for P24.

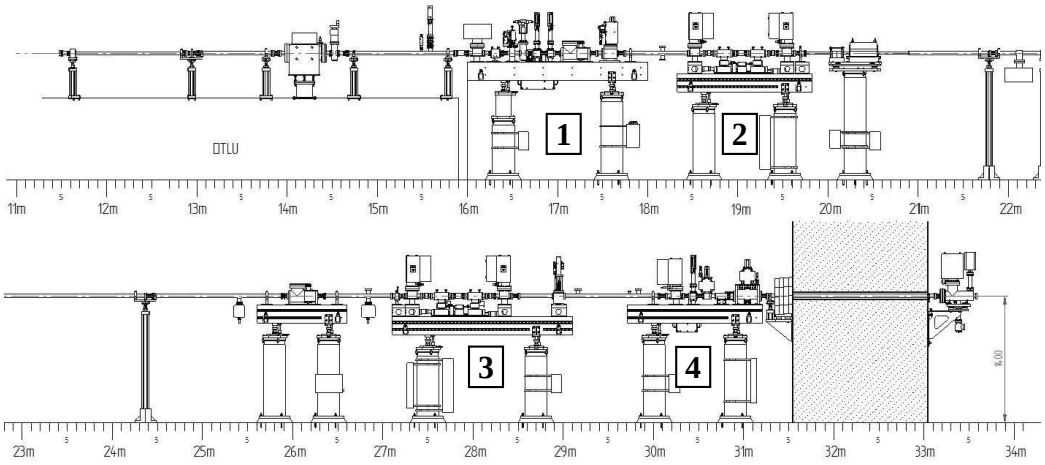

Figure 2.4: Drawing of the beamline front end. The front end consist of four girders with the following components: Resididual gas X-BPM and fast acting valve (1), vertical slit (2), vertical-horizontal slit and filter bank (3), sacrificial absorber and beam shutter (4).

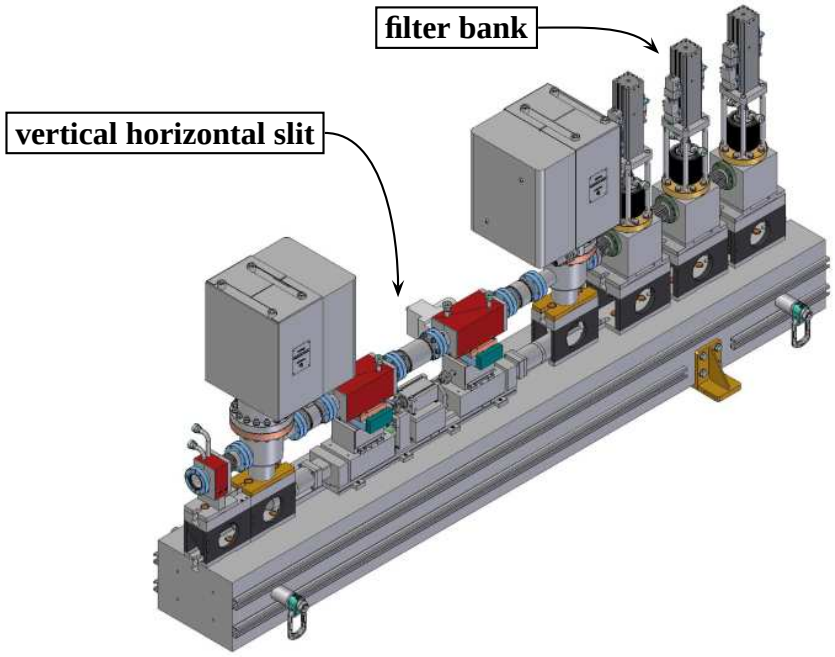

Figure 2.5: Detailed drawing of the third girder with the 'filter bank'. This filter bank will be used for the Cu attenuators.

2.2 Optics

The first optical element of the beamline are the Cu attenuators (see Fig. 2.5), which are in fact water cooled diamond windows, which are plated with $25\mu m$ Cu on both sides. These attenuators are a part of the beamline front end. One attenuator is always in the beam, two are removable and can be inserted if necessary. The required number of attenuators depends on the selected energy. These attenuators act as a high pass filter. The next element is a low pass filter, which consists of two plane mirrors. Together this band pass filters reduce the heat load on the first crystal of the monochromator to a tolerable value. Behind the double crystal monochromator (DCM) a compound refractive lens (CRL) system can be used for focussing. A sketch of this layout is shown in Fig. 2.6 together with a CAD drawing of the instrumentation inside the optics hutch. The CRL system is not shown in the drawing, as it will not be available from the beginning. After the monochromator a sufficient long ($3.7m$) tube is installed as a place holder.

In the following text the optical elements will be described in detail.

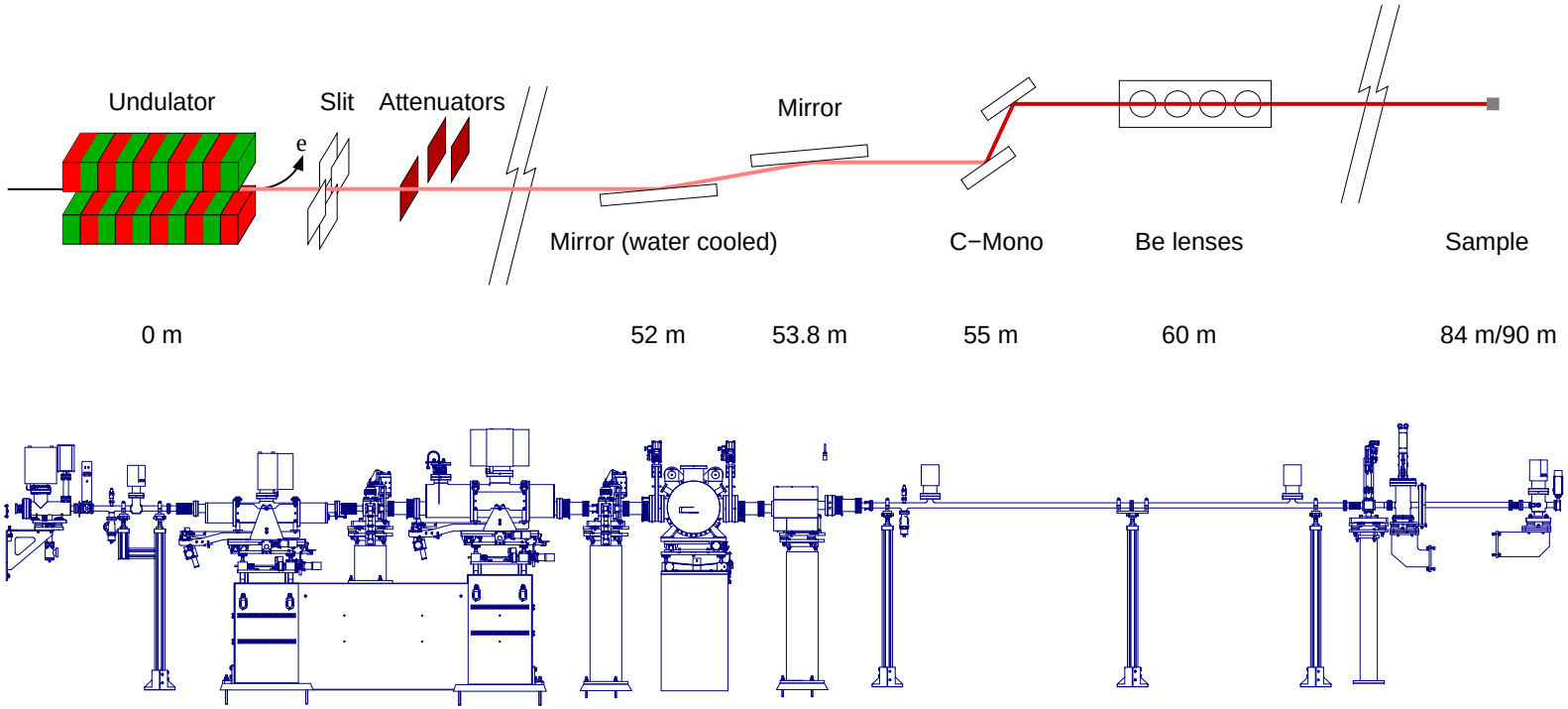

Figure 2.6: Sketch of the beamline layout with approximate postions of optical elements (top) and drawing of the instrumentation, which will be installed inside the optics hutch (bottom). The Be-CRLs are not shown in the drawing.

2.2.1 Mirrors

Two plane mirrors will be used to cut off higher harmonics radiation. The first mirror will be water-cooled and absorbs the heat load originating from the higher harmonics of the undulator. This requires the correct choice of glancing angle so that the critical energy is in between the monochromator energy and the next higher undulator harmonic. In combination with the Cu attenuators the power load on the first DCM crystal can be reduced to values below $2W/mm^2$. As the main part of the heat load is already absorbed by the first mirror, the second mirror does not need water cooling. Its main purpose is to deflect the beam back to a horizontal direction and to further improve rejection of the third harmonic of the DCM energy.

To cover the energy range between $8keV$ and $44keV$ with optimal reflectivity the plane mirrors will be coated with different materials. At lower energies reflectivities of $\approx 95\%$ can be obtained with Rh coating. Above the Rh K absorption edge ($23.2keV$) a different coating has to be used. At this higher energy range reflectivities of $\approx 90\%$ can be obtained with a Pt coating (see Fig 2.7). Thus it is proposed to use two mirrors with two stripes of different coating, Rh and Pt. The uncoated region between these stripes can be used as well to obtain good reflectivities at energies below $8keV$. This might be useful at a later date, e.g. after a monochromator upgrade.

For the above mentioned energy range the angle of incidence has to be varied between $1.5mrad$ and $3mrad$. For potential future upgrade that will allow higher energies (e.g. change of one crystal pair in the DCM) it is planned to allow $1mrad$ as lowest angle of incidence. The horizontal distance of the two mirrors is $1.8m$. This will cause a vertical offset of the beam of $3.6mm$ to $10.8mm$, which has to be compensated by the DCM.

In order to minimize mechanical vibrations both mirror chambers will be mounted on one big granite stone (see Fig. 2.6, bottom).

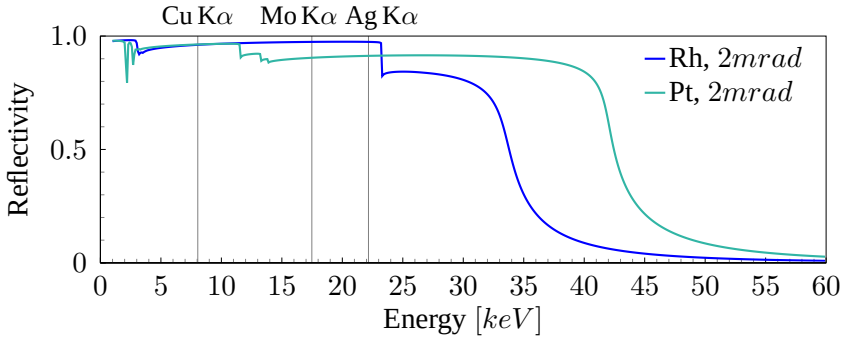

Figure 2.7: Reflectivity curves for Rh and Pt coated mirrors.

2.2.2 Double crystal monochromator

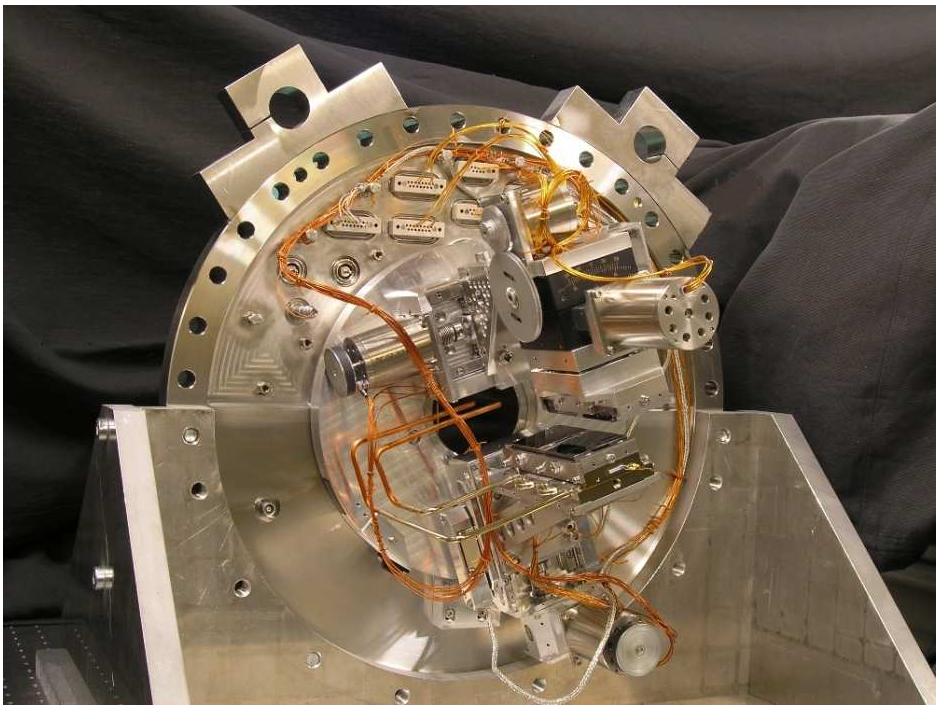

Figure 2.8: C-type DCM without vacuum tank

The new beamline will be equipped with one of the approved water cooled fixed exit double crystal monochromators (see figure 2.8) that were used for powder diffraction at beamline B2 and EXAFS spectroscopy at beamlines C and A1 (C-type DCM). Table 2.2 gives an overview of the relevant parameter of the DCM. Two crystal pairs, a Si(111) and a Si(311), will be installed in the DCM to cover the energy range between $2.4keV$ and $44keV$ (Rickers et al. 2007, Welter, 2010).

DCM type	Fixed exit, 6 - 25 mm offset
DCM crystals	2 pairs, Si(111) and (311), $40 \cdot 40$ mm^2
DCM cooling	Water
Maximum integral power load	30 W
Maximum power load density (normal incidence)	2 W/mm^2

Table 2.2: Properties of the C-type DCM.

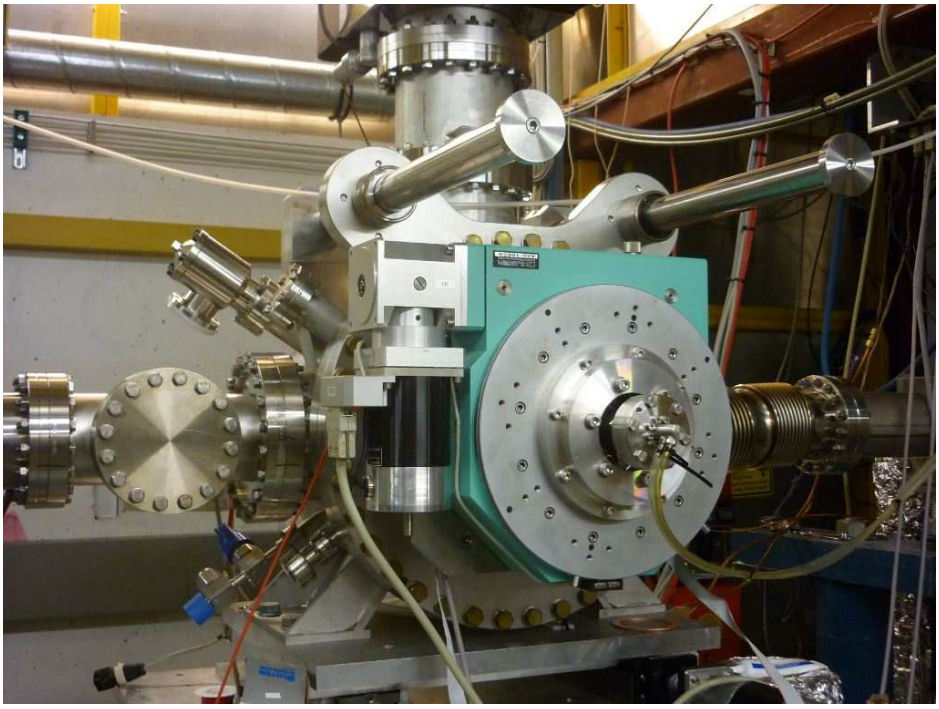

Figure 2.9: C-type DCM installed at beamline BW1 for heat load test (October 2012).

If higher energies might be required in the future, the Si(311) crystal pair could be replaced by a Si(511) crystal pair to allow energies up to $66keV$.

The maximum allowed power load has to be considered in the design of the source (see 2.1). At DORIS III beamline A1 the maximum power density at an incidence angle of $90°$ was $0.7W/mm^2$. The integral power load on the first crystal was estimated to be 21 W. Under these conditions the C-type DCM showed an excellent reproducibility of the energy scale and even after the significant change of the storage ring current after an injection, no influence of the varying power load on the rocking curve position or width (Welter, 2010). Before the shutdown of DORIS III a heat load test with C-type DCM was conducted at the undulator beamline BW1 (see Fig. 2.9) to simulate beam conditions more comparable to a PETRA III undulator. Up to $4W/mm^2$ no degradation of energy resolution was observed.

The beamline design will reserve enough space to replace the C-type DCM with a cryogenically cooled high power load DCM at a later date. For such an upgrade the higher harmonic rejection mirrors will be moved downstream of the monochromator and the Cu attenuators in the front end will be removed.

Operation mode	focal length	N at 44 keV	vertical beam size (FWHM)
Collimating	$60m$	24	$560\mu m$
Focus in P24.2	$17m$	84	$6.1\mu m$
Focus in P24.3	$20m$	71	$7.5\mu m$

Table 2.3: Required focal length, number of Be-lenses with $R = 500\mu m$ and vertical beam size.

2.2.3 Focussing

The unfocussed beam profile shown in Fig. 2.2 has a FWHM of $1.5 \cdot 0.7mm^2$ and a full width at 90% of the maximum of $0.6 \cdot 0.3mm^2$. This already fulfills the largest beamsize requirement (see Table 1.2). This beamsize is also comparable with the beamsize, which was available at beamlines D3 and F1. Because this beam is already sufficient for many experiments, focussing will not be available on day one, but will be commissioned soon. Sufficient space is reserved in the optics hutch at $60m$ downstream of the source for the installation of a Beryllium CRL system. The advantage of a CRL system is that different focal lengths can be easily realized by changing the number of lenses. This allows to realize the different beam sizes in the two experimental stations. An overview is given in Table 2.3. The number of required lenses N for a certain focal length f can be with the lensmaker equation $f = R/2N(1-n)$ and depends on the radius R and the refractive index n. The FWHM of the beam at the CRL system is $\approx 560\mu m$, thus a radius of $R = 500\mu m$ is planned. As the refractive index is approaching 1 with increasing energy, the number of required lenses is also increasing and the maximum number of lenses is required at the highest possible energy $44keV$.

As the highest number of lenses is 84, a binary system with stacks of 1, 2, 4, 8, 16, 32 and 64 lenses is proposed. Such systems are commercially available (e.g. from JJ X-ray). Intermediate beam sizes can be obtained by focussing to a position behind the experimental hutches.

2.3 Experimental hutches

The experimental hutches will provide enough space for all kinds of experiments, even with the large experimental set-ups usually needed for in-situ experiments. A sample preparation room adjacent to the experimental hutches will allow the users to prepare and condition their samples and to measure them without delay.

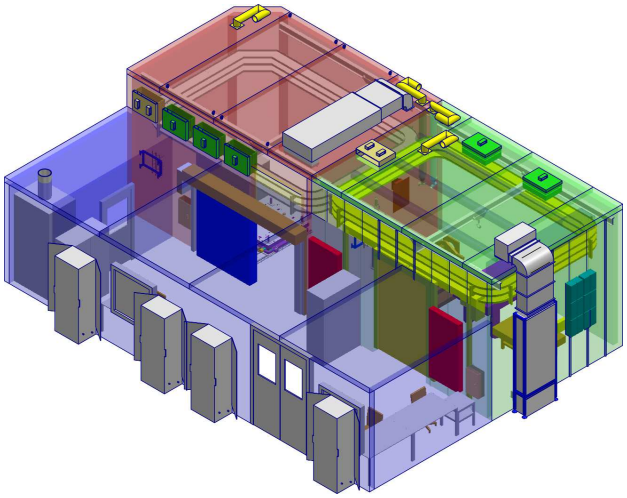

Figure 2.10: CAD drawing of the experimental hutches

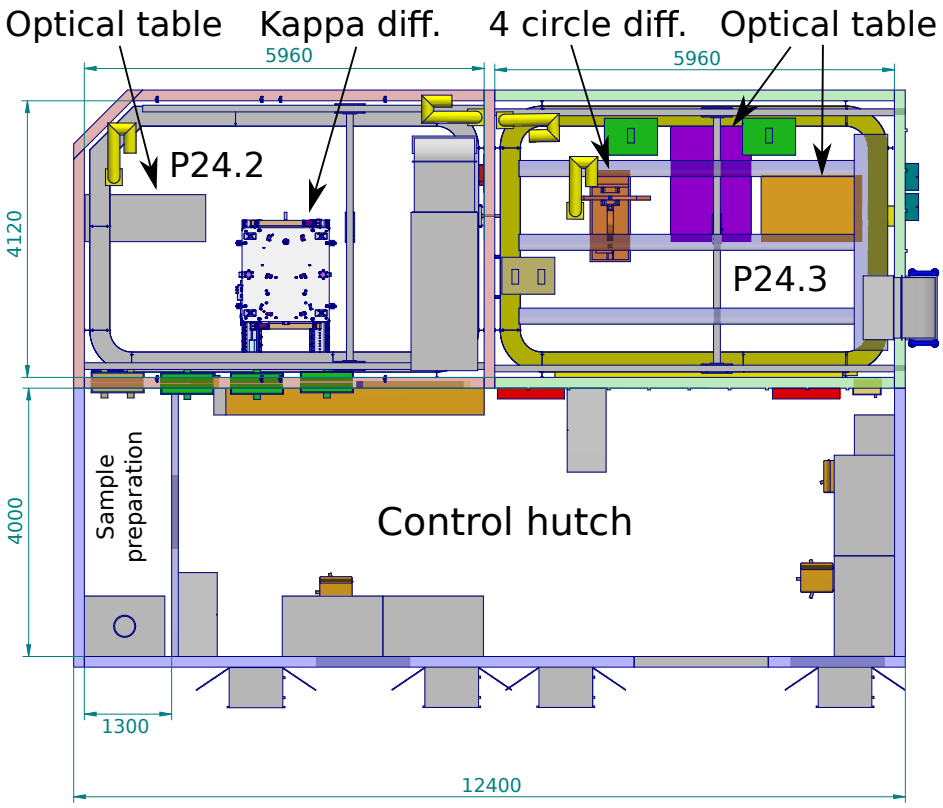

Figure 2.11: Floor plan of the experimental hutches

2.3.1 First experimental hutch (P24.2)

With respect to the potential applications and various sample environments, the basic design of the new diffractometer was defined in Kappa-geometry to offer as much flexibility in reciprocal space as possible. It should provide a motorised xyz-stage able to carry sample loads up to 10 kg. Two independent detector circles with integrated translation stages should be designed to take loads of 30 kg. The design should offer easy exchange and combination of different detectors (e.g. Pilatus 1M, CCD, polarisation analyser), sample environments (cryostats, heaters), laser systems for pump and probe experiments or high-resolution polarising digital sample microscopes. A european call for tenders with detailed specifications (Table 2.4) was placed in January 2012 and the final order in summer 2012. The diffractometer was delivered in December 2013 and preliminary installed in the former DORIS III experimental hall (see Fig. 2.12). Currently, final testing and commissioning is in progress and operation with a Mo microsource for diffraction experiments is expected to start in summer 2014. The relocation to PETRA III hall east is planned for summer 2015.

Diffractometer circles	
Min. step size (2θ, ω)	$5 \cdot 10^{-5}\,\circ$
Min. step size (κ, ϕ)	$5 \cdot 10^{-4}\,\circ$
Accuracy (2θ)	$2 \cdot 10^{-3}\,\circ$
Accuracy (ω)	$2 \cdot 10^{-4}\,\circ$
Accuracy (κ, ϕ)	$8 \cdot 10^{-3}\,\circ$
Repeatability (2θ, ω)	$2 \cdot 10^{-4}\,\circ$
Repeatability (κ, ϕ)	$3 \cdot 10^{-3}\,\circ$
Detector translations	
Range	$500mm$
Min. step size	$0.001mm$
Accuracy	$20\mu m$
Repeatability	$12\mu m$
Support table	
Translation range x	$+100/-500mm$
Translation range z	$\pm 60mm$
Accuracy/repetability	$2\mu m$
XYZ-stage	
Free distance	$190mm(250mm)$
Range x/y	$\pm 25mm$
Range z	$\pm 12.5mm$
Min. step size (xyz)	$0.25\mu m$
Accuracy (xy/z)	$2\mu m/20\mu m$
Repeatability (xy/z)	$2\mu m/20\mu m$
Load (Max.)	
Detector	$30kg$
XYZ-stage	$10kg$
SOCs (Tender specifications)	
$\omega/\kappa/\phi$ 5 kg	$30\mu m$
$\omega/\kappa/\phi$ 10 kg	$45\mu m$
$\omega/\kappa/\phi$/xyz 5 kg	$50\mu m$
$\omega/\kappa/\phi$/xyz 10 kg	$70\mu m$

Table 2.4: Detailed Kappa diffractometer specifications

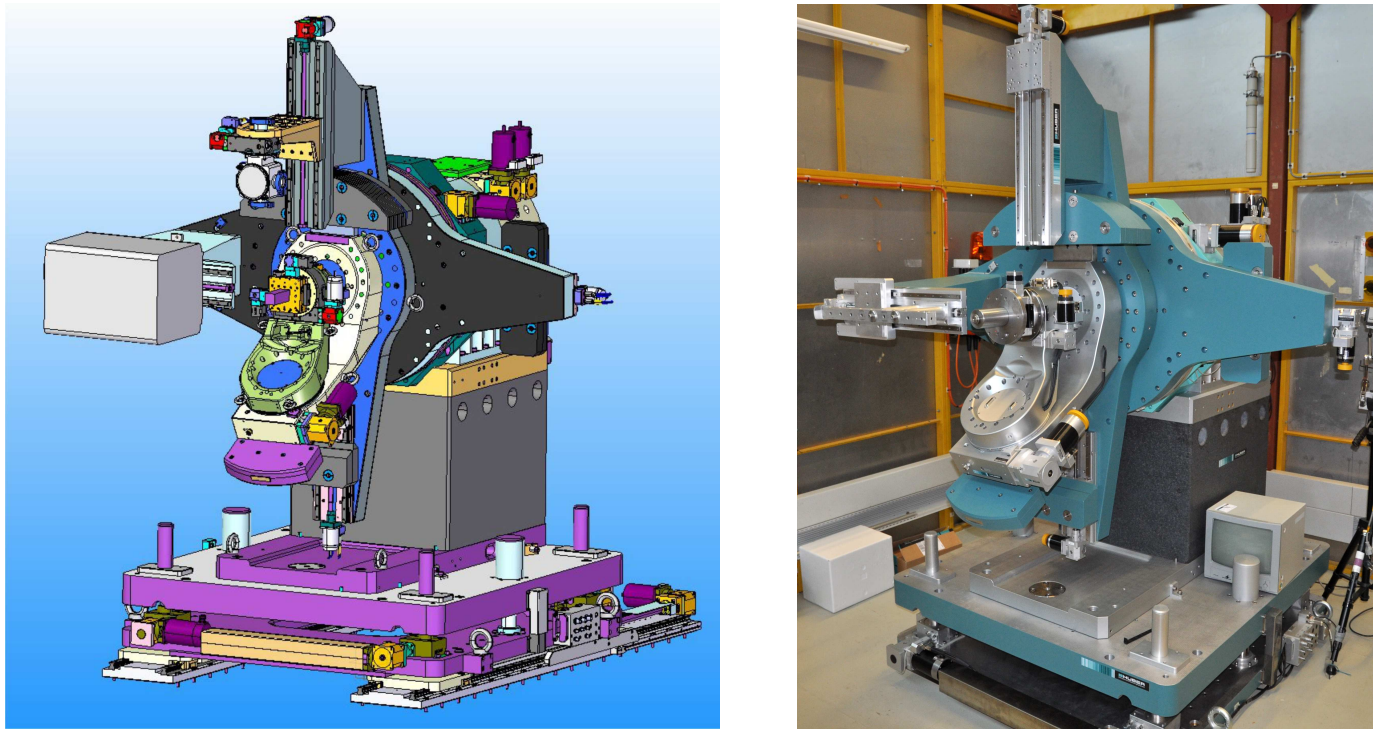

Figure 2.12: The new Kappa diffractometer: CAD drawing (left) and after delivery in December 2013 (right).

Further BMBF project funded hardware and developments

In addition to the Kappa-diffractometer, a variety of additional experiment hardware components were supplied by the BMBF project members during the first and second funding period. A special polarisation analyser (Huber) several detectors with counting electronics like $LaBr_3$ scintillation counters, a silicon drift detector (KETEK) and a PIN diode are supplied. For high-temperature investigations in reflection geometry an Anton Paar oven is available apart from already existing HT devices which are currently further optimised (remote control, stability). With respect to sample manipulation and analysis a combination of a high-resolution digital polarising microscope system with a precise xyz-stage has been already successfully tested at DORIS III (beamline F1). Aiming to high-resolution sample manipulation including combined tilt and rotation movements in the sub-micrometer scale beyond the Kappa-diffractometer specifications, a small hexapod system (PI 811) is available and already adapted to the diffractometer sample stage. Apart from these main components a range of further hardware (piezo/standard positioning devices, vacuum high-precision slits) were purchased for primary beam conditioning. Current developments include a milli-second shutter system, primary beam collimating system, 4-quadrant beam-position monitor and slit systems. Regarding safe user operation, a light-barrier based anti-collision device for area detectors is under development.

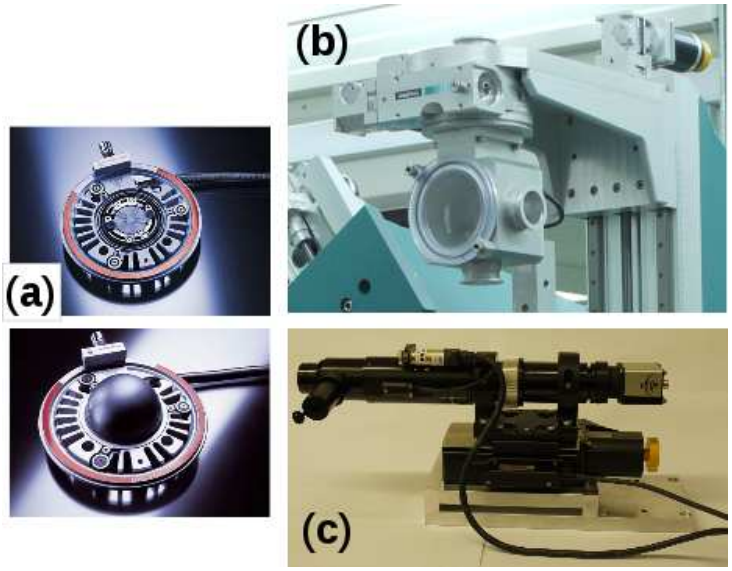

Figure 2.13: Selected additional experiment components: (a) high temperature oven (b) polarization analyzer (c) high resolution polarizing microscope.

2.3.2 Second experimental hutch (P24.3)

As counterpart to the Kappa-diffractometer, which will be installed in hutch P24.2, a four circle diffractometer with Eulerian cradle will be installed in hutch P24.3. This way the user can choose between two different geometries and select the one that is best suited for their experiment. It is planned to install the Huber four circle diffractometer, which was in use at beamline D3, in P24.3 after it has been refurbished by the manufacturer.

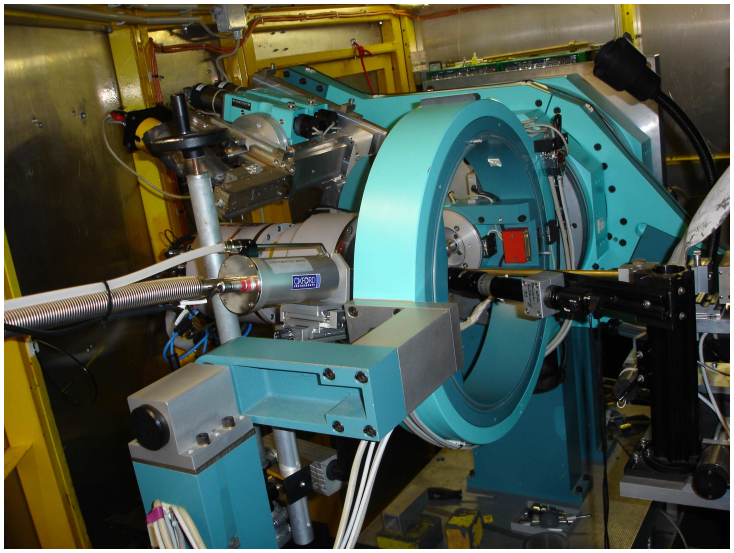

Figure 2.14: 4-circle diffractometer with Eularian cradle at former DORIS III beamline D3.

Besides some minor necessary repairs and a general realignment of the diffractometer circles, the following improvements of the diffractometer are planned:

- Replacement of the old Berger-Lahr stepper motors by high resolution stepper motors, in order to reach a resolution of $10^{-4}\,\circ$
- Installation of a motorized detector stage (for area detector)
- Redesign of the counterweight

The main application of P24.3 will be measurements in a closed cycle cryostat (re-used from beamline D3, temperatures from $8K$ up to $325K$). For this cryostat a special xyz-stage with micrometer precision is available. As the sample will be mounted inside two Beryllium domes, a collimator in front of the detector is needed to reduce the background. This implies the use of a point detector. For this purpose different fast point detectors with deadtime $< 1\mu s$ will be provided (see Table 2.5).

Figure 2.15: Helium and Nitrogen gas jet cryostat (Cryocool G2b-LT) consisting of the gas jet nozzle with alignment stage (left) and Gifford-McMahon cooler with heat exchanger (right). The Helium compressor for GM cooler is not shown.

For low temperature measurements with 2D detector a gas jet cryostat will be available (see Fig. 2.15). The nozzle of this device can be mounted on the diffractometer in such a way that the gas jet is parallel to the ω axis. This way and because of the small size of the nozzle the angular degrees of freedom will be limited only marginally. This cryostat can be used with Helium (for $10K$–$\approx 200K$) or Nitrogen (for $\approx 100K$–$300K$). The selected gas is cooled with a heat exchanger that is mounted on a closed cycle Gifford-McMahon cooler. Instead of liquid Helium or Nitrogen it uses compressed gas as supply. The gas jet cryostat can also be used in P24.2. As 2D detector a MarCCD 165 will be available at the beamline. Alternatively different detectors (e.g. Pilatus) can be borrowed from the detector pool.

Another application of P24.3 will be measurements at high pressure with diamond anvil cells (DACs). Due to the large angular degree of freedom the four circle diffractometer from D3 is very well suited for this type of experiments.

In addition to the diffractometer two optical tables (see Fig. 2.11, right) will be installed inside P24.3. These tables will be initially used for a X-ray free electron laser oscillator (XFELO) test setup. Later, they can be also used for complex user experiments that require additional space, e.g. laser pump-probe measurements. A laser safety interlock system will be installed for this hutch.

2.4 Summary

A summary of the beamline parameters is shown in Table 2.5.

Beamline parameter	**User demand**
Energy range	8keV (fixed) and 15keV – 44keV (tunable)
Photon flux at sample at $22.162keV$	$10^{12}s^{-1}$ with Si(311) monochromator
Vertical beamsize (FWHM)	unfocussed $700\mu m$ collimated $560\mu m$ micro down to $6\mu m$
Temperature range	$8K$ – $1373K$
Detectors	• MarCCD 165 • $LaCl_3$ and $LaBr_3$ scintillation counter • Avalanche photo diode • Split ion chamber (beam position monitor) • 2 Silicon drift detectors • Pilatus (from detector pool)
Experimental hutches	• Two separate hutches • Shared control hutch with sample preparation lab • Helium and Nitrogen supply for gas jet cryostats

Table 2.5: Summary of beamline parameters

Milestone	**Date**
Beamline advisory committee meeting	July 2, 2014
Design of experimental hutches finalized	August 2014
Optics hutch constructed	February 2015
Optics installed	September 2015
Experimental hutches constructed	July 2015
Instruments installed	November 2015
Front end installed	January 2016
Start of beamline commissioning	February 2016
First experiments	May 2016

Table 2.6: Time plan